

MYD88 L265P Lymphoma Cells Induce the Disruption of Brain Microvascular Endothelial Cells Barrier *via* Activating NLRP3 and NF- κ B Pathway

XIN DAI, Y. YUAN, K. WU, SHU WANG, HUA JIANG¹ AND T. CHEN*

Department of Hematology, Huashan Hospital, Shanghai 200040, ¹Department of Gynecology, Obstetrics and Gynecology Hospital, Fudan University, Shanghai 200011, China

Dai *et al.*: Brain Microvascular Endothelial Cells Barrier Disruption

Myeloid differentiation primary response 88 L265P was a functional mutant currently found in hematological tumors, especially occurred frequently in central nervous system lymphomas. The integrity of the blood brain barrier was critical to maintain the normal microenvironment in the brain. Blood brain barrier prevented neurotoxic plasma components, blood cells and pathogens from entering the brain. However, the molecular crosstalk between blood brain barrier and lymphoma cells required further investigation. In this study, human brain microvascular endothelial cells were used to simulate a blood-brain barrier model *in vitro*. It was found that the myeloid differentiation primary response 88 L265P lymphoma cells disrupted the function of brain microvascular endothelial cells barrier by the decrease of transepithelial electric resistance value, destruction of tight junction and increase of leukocyte adhesion molecules. These processes were achieved by activating NLR family pyrin domain containing 3 and nuclear factor kappa B pathway in brain microvascular endothelial cell. In addition, when Myeloid differentiation primary response 88 L265P lymphoma cells was treated with ibrutinib, there was no significant change on the permeability and integrity of the brain microvascular endothelial cell barrier.

Key words: Myeloid differentiation primary response 88 L265P mutation, lymphoma, blood brain barrier, ibrutinib

Oncogenic Myeloid Differentiation Primary Response 88 (MYD88) L265P mutant in Diffuse Large B Cell Lymphoma (DLBCL), had been identified in 2011^[1]. Subsequently, MYD88 L265P had been identified in numerous other Non-Hodgkin Lymphoma (B-NHL) subtypes, especially in Waldenström's Macroglobulinemia (WM) and Primary Central Nervous System Lymphoma (PCNSL). In addition, its occurrence was shown to be an early, clonal event in Chronic Lymphocytic Leukemia (CLL). MYD88 mutations in cancers mostly occurred in exons 3, 4 and 5 as a single base substitution at c.794T >C resulting a L265P amino acid change in the Toll/Interleukin (IL)-1 receptor domain^[2].

The MYD88 L265P mutation occurred at high frequency in Central Nervous System (CNS) lymphoma and was extremely rare in non-hematologic malignancies. The MYD88 L265P mutation was

reported 2103 times in the COSMIC database. Out of 2103 reports, 2097 cases were in hematologic malignancies, with rare instances in lung (n=2), prostate tumors (n=1), large intestine (n=1) and peritoneum (n=1). In DLBCL, the MYD88 L265P mutation had been related to specific extra nodal sites (particularly the so-called immune-privileged territories), such as brain and testis^[3,4]. Lymphoma of the CNS included two major subtypes; PCNSL arisen and confined to the CNS and Metastatic (or secondary) CNS Lymphoma (MCNSL), which originated at sites outside the CNS^[5]. PCNSL and MCNSL were rare CNS malignancies that exhibited aggressive clinical behavior and poor prognosis. Whole exome and targeted sequencing studies had determined the genetic profiles of PCNSL. Notably, mutations in genes associated with Nuclear Factor Kappa B (NF- κ B) and B-Cell Receptor (BCR) signaling pathways were highly frequent in PCNSL. In particular, the

*Address for correspondence

E-mail: medfudan2017@126.com

MYD88 L265P mutation was found in about 38 %-85.4 % of PCNSL patients but never in those with non-hematological brain tumors, suggesting that this mutation was useful for differential diagnosis of PCNSL among CNS tumors^[6-12]. Fukumura *et al.*^[10] found that MYD88 mutations could be detected in about 86 % PCNSL cases and was present in Peripheral Blood Mononuclear Cells (PBMCs) from one quarter of MYD88 mutation-positive PCNSL patients. Zorofchian *et al.*^[2] detected the MYD88 L265P mutation in the Cerebrospinal Fluid (CSF) of a patient with MCNSL. They found MYD88 L265P mutation from Formalin Fixed Paraffin Embedded (FFPE) tissue obtained from the brain biopsy and circulating tumor Deoxyribonucleic Acid (ctDNA) obtained from the CSF (CSF-ctDNA). In contrast, the V217F mutation was not found either in the tissue or in the CSF-ctDNA. The prognostic relevance of MYD88 mutations in DLBCL was still a matter of debate. Dubois's study supported that the MYD88 L265P variant alone was not an independent prognostic factor in ABC DLBCL, but suggested that MYD88-mutant DLBCL cases were significantly more likely to experience CNS relapse than MYD88 WT cases^[13].

The function of Blood Brain Barrier (BBB) was separated neural tissue from circulating blood. The BBB comprised of a single layer of endothelial cells, which build the walls of blood vessels and display unique cell biological characteristics. CNS endothelial cells had specialized Tight Junctions (TJs) to prevent free bystander cells pass through the vessel wall and low expression levels of Lipoarabinomannan (LAM) to limit immune cells enter the brain. These characteristics distinguished CNS endothelial cells from peripheral endothelial cells^[14]. In disease states, BBB was broken down and dysfunctional, which lead to cytokines, chemokine's and peripheral leukocytes enter the CNS and accelerated disease progression^[15]. Rochfort *et al.*^[16] demonstrated that Tumour Necrosis Factor-alpha (TNF- α) increased endothelial cells permeability in part *via* Reactive Oxygen Species (ROS) mediated down-regulation of inter endothelial junction proteins such as ZO-1, occludin, claudin-5, and VE-cadherin.

Most studies in the field of the interaction of tumor cells and the BBB have mainly focused on solid tumors such as glioma, lung cancer, breast cancer and also on acute lymphoblastic leukemia. Brain metastases in non-hematological malignancies

usually associate with poor survival outcomes and pose distinct clinical challenges^[17]. Previous published studies indicated that there were different tumor cells subpopulations with different affinities to colonize certain target organs, depending on their genetic constitution^[18]. Tumor cells that overexpressed the Chemokine Receptor-4 (CXCR4), Parathyroid Hormone-Like Hormone (PTHrH), IL-11, Matrix Metalloproteinase-1 (MMP1) and Osteopontin (OPN) genes had the ability to promote bone metastases^[18], while cells that overexpressed Cyclooxygenase (COX), epiregulin and Angiopoietin-Like 4 (ANGPTL4) exhibited a tropism for the lung^[19]. In addition, tumor cells overexpressed ST6GALNAC5, COX-2, Heparin-Binding-Epidermal Growth Factor (HB-EGF) and ANGPTL4 had a particular affinity for colonizing the CNS^[20]. Presumably, the gene patterns specific to each of these cell subpopulations may be obtained through a series of somatic changes^[18].

In our study, we intended to clarify whether the MYD88 L265P lymphoma cells destroy the brain microvascular endothelial cells barrier by activating NLR Family Pyrin Domain Containing 3 (NLRP3) and NF- κ B pathway. After treating lymphoma cells with ibrutinib, whether there were still significant changes on the permeability and integrity of the brain microvascular endothelial cells barrier.

MATERIAL AND METHODS

Cell culture:

SUDHL-4 cells were obtained from the Shanghai Institute for Biological Sciences. U2932 were obtained from the DSMZ. SUDHL-4 and U2932 maintained in Iscove's Modified Dulbecco's Medium (IMDM) supplemented with 10 % Fetal Bovine Serum (FBS) in the presence of 1 % penicillin/streptomycin/amphotericin B (all from Gibco, United States of America (USA)). Human brain microvascular endothelial cells, hCMEC/D3 cells were obtained from the American Type Culture Collection (ATCC), ATCC were cultured in Endothelial Cell Basal Medium-2 (EBM-2) (Lonza, Swiss) supplemented with 5 % FBS (Sigma, USA), 5 mg/ml ascorbic acid (Sigma, USA), 1 ng/ml basic Fibroblast Growth Factor (bFGF) (Sigma, USA), 0.2 % EGF (Sigma, USA), 0.2 % Vascular Endothelial Growth Factor (VEGF) (Sigma, USA), 0.2 % gentamycin (Invitrogen, USA), and 1 % penicillin/streptomycin (Gibco, USA). The proliferation ability

of hCMEC/D3 was measured by Cell Counting Kit-8 (CKK-8) assay (Dojindo, Mashikimachi, Japan) according to the manufacturer's instruction.

Plasmid constructs virus production and transfection:

Human MYD88 complementary DNA (cDNA) was consistent with NM-002468 (L265P) mut and sub cloned into the lentiviral expression vector GV492-gcGFP-Puro (Jikai, Shanghai, China). The mutations resulting in L265P substitutions were introduced into MYD88 coding sequence by site-directed mutagenesis and confirmed by full-length DNA sequencing. Lentiviral supernatants were generated by co-transfection of lentiviral packaging plasmids and expression vector into 293T cells, harvested at 72 h post-transfection. The supernatants were then concentrated and purified by centrifuge for 2 h. SUDHL-4 and U2932 cells were infected with the concentrated lentiviral supernatants (Multiplicity of Infection (MOI)=10). The expression of Green Fluorescent Protein (GFP) was analyzed by micropublisher 3.3 RTV (Olympus, Japan) and qualitative Polymerase Chain Reaction (qPCR). Transduced SUDHL-4 and U2932 cells were selected in growth media containing 5 µg/ml puromycin (Jikai, Shanghai, China) for 14 d.

Flow cytometer analysis:

Apoptosis Detection (BD, USA) was performed according to the manufacturer's instructions. In brief, a total of 10⁶ hCMEC/D3 cells were resuspended in 100 buffer containing anti-bodies against PE and Annexin V-APC (Kaiji, China) in room temperature for 20 min. Data were acquired within 1 h after staining on a BD LSR Fortessa (BD Biosciences, USA) and all flow cytometry data analysis employed FlowJo software (Ashland, Oregon, USA).

Quantitative Real-time PCR:

HCMEC/D3 cells were harvested for extraction of total Ribonucleic Acid (RNA) and analysis of messenger RNA (mRNA). mRNA was extracted from the samples using TRIzol (Life Technologies, Carlsbad, California, USA) according to the manufacturer's instruction. cDNA was synthesized using the Primer Script RT reagent kit (Takara, Shiga, Japan). Real-time PCR was performed on a step one plus real time PCR System (Life Technologies) with SYBR Green PCR Master Mix (Takara, USA). Each cDNA sample was assayed in triplicate and results were analyzed by the comparative CT method. Beta (β)-actin was routinely used for normalization purposes. The primer sequences used in this study was shown in Table 1.

TABLE 1: PRIMER SEQUENCES FOR RT-PCR

Target	Sequence (5'-3')
β-actin-F	GATTTAAAACTGGAACGGTGAAG
β-actin-R	TAGGATGGCAAGGGACTTCTTG
ZO-1-F	AGCCATCCCGAAGGAGTTG
ZO-1-R	ATCACAGTGTGGTAAGCGCA
Claudin-5-F	AGATTGAGAGGTCTGGGAAGC
Claudin-5-R	TCTTCATCCCATGGCAAACA-3
NF-κB-F	AACAGCAGATGGCCCATACC
NF-κB-R	AACCTTTGCTGGTCCACAT
MYD88-F	CTATTGCCCCAGCGACATCC
MYD88-R	GGCCTTCTAGCCAACCTCTTT
NLRP3-F	ACAATGACAGCATCGGGTGT
NLRP3-R	AGAAAGATAGCGGAATGATGA
GSDMD-F	CAGTTTCACTTTTAGCTCTGGGC
GSDMD-R	CTGGACCACTCTCCGACTA
ICAM-1-F	TCTTCCTCGGCCTTCCATA
ICAM-1-R	AGGTACCATGGCCCCAAATG
VCAM-1-F	GGACCACATCTACGCTGACA
VCAM-1-R	TTGACTGTGATCGGCTTCCC

Western blotting:

Total hCMEC/D3 cells were prepared using Radioimmunoprecipitation Assay (RIPA) buffer, sodium deoxycholate and protease inhibitor cocktail, as well as phosphatase inhibitor cocktail (Beyotime, China). The lysates were transferred into Polyvinylidene Difluoride (PVDF) membranes. The membranes were blocked and incubated with primary antibody at 4° overnight, the corresponding secondary antibody for 1 h at room temperature and then visualized with enhanced chemiluminescence and quantified by densitometry. Scanning densitometry of Western blotting was performed using NIH ImageJ software, with Glyceraldehyde 3-Phosphate Dehydrogenase (GAPDH) routinely employed as a loading control to facilitate densitometric normalization of bands. The following primary antibodies were used to detect proteins of interest: anti-ZO-1 (1:1000, Affinity Biosciences, China), anti-claudin-5 (1:1000, proteintech, China), anti-NLRP3 (1:2000, Adipogen, USA), anti-MYD88 (1:1000, proteintech, China), anti-p-P65 (1:2000, Adipogen, USA), anti-Gasdermin D (GSDMD) (1:1000, proteintech, China), anti-Intercellular Adhesion Molecule-1 (ICAM-1) (1:1000, proteintech, China), anti-Vascular Cell Adhesion Protein 1 (VCAM-1) (1:1,000, Affinity Biosciences, China).

Immunofluorescence detection:

For hCMEC/D3 cells staining, 10^4 cells were cultured

on confocal dish. The fixed cells were stained with anti-ZO-1 (1:1000, Affinity Biosciences, China), anti-CD31 (1:1000, Proteintech, China) and anti-GSDMD (1:1000, proteintech, China).

Statistical analysis:

Results are expressed as mean±standard deviation. All experiments were performed in 3 replicates and in at least 3 independent experiments. The significance of differences was analyzed using Student's t-test. A value of * $p < 0.05$ was considered significant.

RESULTS AND DISCUSSION

HCMEC/D3 cells were used to construct a blood-brain barrier model *in vitro*. The lower chamber simulated the parenchymal side of the brain and the upper chamber simulated the side of the vascular cavity. Considering the successful construction of the *in vitro* BBB model on the 5th d, lymphoma cells were planted in the upper chamber of 5×10^4 cells/well. The Trans Epithelial Electrical Resistances (TEER) value of the hCMEC/D3 (SUDHL-4 L265P) and hCMEC/D3 (U2932 L265P) decreased significantly at 72 h, while neither the NC nor vector groups caused significant changes. The numbers of lymphomas cells SUDHL-4 L265P and U2932 L265P that entered the lower chamber were significantly more than the WT and vector groups as shown in fig. 1A.

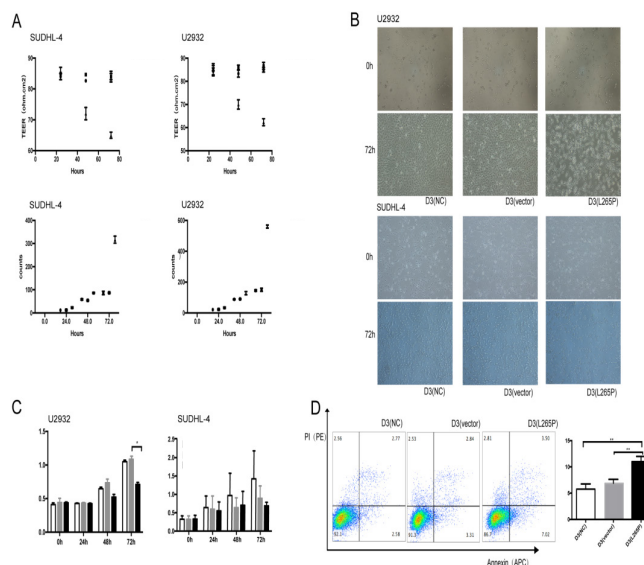


Fig. 1: MYD88 L265P lymphoma cells changed the biological function of hCMEC/D3 cells, (A): The TEER value of the hCMEC/D3 cells (up) and the numbers of lymphomas that entered the lower chamber (down); (B): The morphology of hCMEC/D3 cells under microscope; (C): The proliferation of hCMEC/D3 cells tested by CCK8, * $p < 0.05$ and (D): Flow cytometry to detect apoptosis of hCMEC/D3 cells, ** $p < 0.01$

Note: (A) (●): D3 (NC); (■): D3 (vector); (▲): D3 (L265P); (○): WT; (□): Vector and (▲): L265P and (C) (□): D3 (NC); (■): D3 (vector) and (●): D3 (L265P)

The morphology of hCMEC/D3 cells in MYD88 L265P lymphoma cell groups changed obviously. The shrunk and gap of cells became loose at 72 h (fig. 1B). The proliferation abilities of hCMEC/D3 cells in MYD88 L265P lymphoma cell groups were significantly lower than that in NC and vector groups, and the differences were most significant at 72 h (fig. 1C). In addition, we found that the early apoptosis rate of hCMEC/D3 (U2932 L265P) group was significantly higher than that in the NC and vector groups (fig. 1D). Pyroptosis was a form of cell death caused by inflammatory caspase. GSDMD was direct and final execution in the process of cell pyrolysis^[21]. After 72 h, the GSDMD expression of hCMEC/D3 (SUDHL-4 L265P) was up regulated compared with hCMEC/D3 (SUDHL-4 vector) as shown by the immunohistochemical method (fig. 2A). At the RNA and protein level, the GSDMD expression of hCMEC/D3(U2932 L265P) group were significantly higher than that in the NC and the vector groups ($p < 0.01$, fig. 2A).

ZO-1 and claudin-5 were indispensable for the correct organization of TJs and maintained the integrity of brain microvascular endothelial cells^[22]. They were considered to contribute to the “sealing” of the TJs in modulating BBB permeability^[23]. The results showed that the ZO-1 connection of hCMEC/D3 (SUDHL-4 L265P) was broken, the edges were discontinuity and the fluorescence expression was significantly lower than hCMEC/D3 (SUDHL-4 vector). At the RNA

and protein level, the ZO-1 and claudin 5 levels of hCMEC/D3 (U2932 L265P) group were lower than that of NC and vector groups ($p < 0.01$, fig. 2B).

Another feature of CNS endothelial cells was the low expression of LAMs, which restricted immune cells from entering the brain. In addition, the surface expression of adhesion molecules in endothelial cells, including VCAM-1 and ICAM-1, maintained a permanent state of chronic inflammation and promote endothelial dysfunction^[24]. Interestingly, we found that the expression of ICAM-1 and VCAM-1 in the hCMEC/D3 (L265P) groups were up-regulated at the RNA and protein level (fig. 2C). The result suggested that MYD88 L265P lymphoma cells created favorable conditions for them to cross the endothelial cells barrier.

The NF- κ B played a key role in the survival and proliferation of cells. Moreover, NF- κ B activation contributes to inflammatory reactions by regulating pro-inflammatory cytokine generation and leukocyte recruitment, which also aggravates endothelial dysfunction^[25]. In the nucleus, NF- κ B promoted the transcription of NLRP3, whose activation invokes endothelial dysfunction^[26]. We found that hCMEC/D3 (SUDHL-4 L265P) at the RNA level and hCMEC/D3 (U2932 L265P) at the protein level had higher expression of NLRP3, NF- κ B and caspase-1 compared with NC and vector groups ($p < 0.05$, fig. 2D).

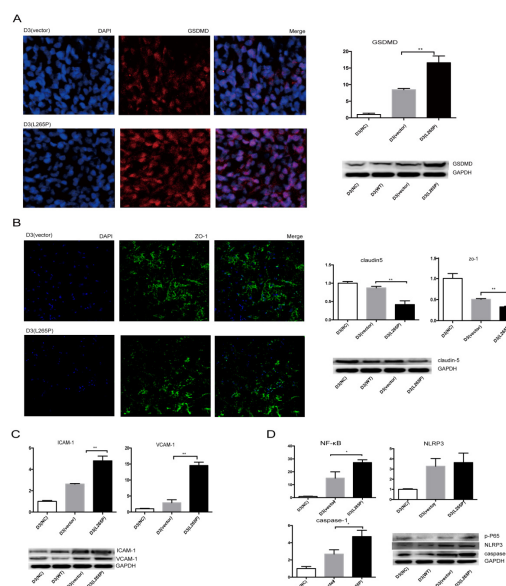


Fig. 2: MYD88 L265P lymphoma cells changed the characteristic of hCMEC/D3 cells, (A): Immunofluorescence, RT-PCR and Western blotting analysis of GSDMD in hCMEC/D3 cells for 72 h; (B): Immunofluorescence analysis of ZO-1, RT-PCR analysis of ZO-1 and claudin-5 and Western blotting analysis of claudin-5 in hCMEC/D3 cells for 72 h; (C): The RT-PCR or Western blotting analysis of ICAM-1 and VCAM-1 in hCMEC/D3 cells and (D): RT-PCR or Western blotting analysis of NF- κ B, NLRP3 and caspase-1 in hCMEC/D3 cells
Note: ** $p < 0.01$, *** $p < 0.001$, * $p < 0.05$ and ** $p < 0.01$ and *** $p < 0.001$

Ibrutinib was a first-class oral inhibitor of Bruton's Tyrosine Kinase (BTK), which integrated BCR and Toll-Like Receptor (TLR) signaling^[27,28]. We treated lymphoma cells with ibrutinib (25 μ M, 6 h). The TEER value of the hCMEC/D3 (SUDHL-4 L265P-ibrutinib) and hCMEC/D3 (U2932 L265P-ibrutinib) were significantly higher than that in L265P groups at 72 h, while there was no difference with NC groups. The numbers of lymphomas cells SUDHL-4 L265P-ibrutinib and U2932 L265P-ibrutinib that entered the lower chamber were significantly less than L265P groups, while there was no difference to group WT and vector (fig. 3A). There was significant morphology changes observed in hCMEC/D3 (L265P-ibrutinib) groups compared to L265P groups, while no change was observed with NC groups (fig. 3B). The proliferation abilities of hCMEC/D3 (U2932 L265P-ibrutinib) were significantly higher than hCMEC/D3 (U2932 L265P) and the differences were most significant at 72 h. In addition, the early apoptosis rate of hCMEC/D3 (U2932 L265P-ibrutinib) group was significantly lower than hCMEC/D3 (U2932 L265P). The GSDMD expression of hCMEC/D3 (SUDHL-4 L265P-ibrutinib) was down regulated compared with hCMEC/D3 (SUDHL-4 L265P) as shown by the immunohistochemical method (fig. 4A). At the RNA and protein level, the GSDMD expression of hCMEC/D3 (U2932 L265P-ibrutinib) group was lower than hCMEC/D3 (U2932 L265P) group. Similarly, the changes of proliferation abilities, early apoptosis rate and GSDMD expression were

not found between L265P-ibrutinib groups and NC groups (fig. 3C-fig. 3D and fig. 4A). The ibrutinib inhibited the effects of L265P mutation in lymphoma cells on the TEER value, morphology changes, proliferation and apoptosis abilities, and GSDMD expression of hCMEC/D3 cells as shown in fig. 3A-fig. 3D and fig. 4A

Interestingly, the ZO-1 connection of hCMEC/D3 (U2932 L265P-ibrutinib) was integrity and the expression of ZO-1 was up-regulated compared with hCMEC/D3 (U2932 L265P) as shown by the immunohistochemical method (fig. 4B). At the RNA and protein level, the ZO-1 and claudin 5 expression of hCMEC/D3 (U2932 L265P-ibrutinib) group were higher than hCMEC/D3(U2932 L265P) group, while no difference was found compared with NC groups (fig. 4B). The ICAM-1 and VCAM-1 expression in the hCMEC/D3 (L265P-ibrutinib groups were down-regulated at the RNA and protein level than hCMEC/D3 (L265P groups (fig. 4C). These results suggested that ibrutinib made the MYD88 L265P lymphoma cells lose the ability to attach the endothelial cell barrier and disrupt its integrity. Moreover, hCMEC/D3 (U2932 L265P-ibrutinib) had lower expression of NLRP3, NF- κ B and caspase-1 compared with L265P group at the RNA and protein level (fig. 4D). This result indicated that the MYD88 L265P lymphoma cells treated with ibrutinib no longer had the ability to activate NLRP3, caspase-1 and NF- κ B of hCMEC/D3 cells.

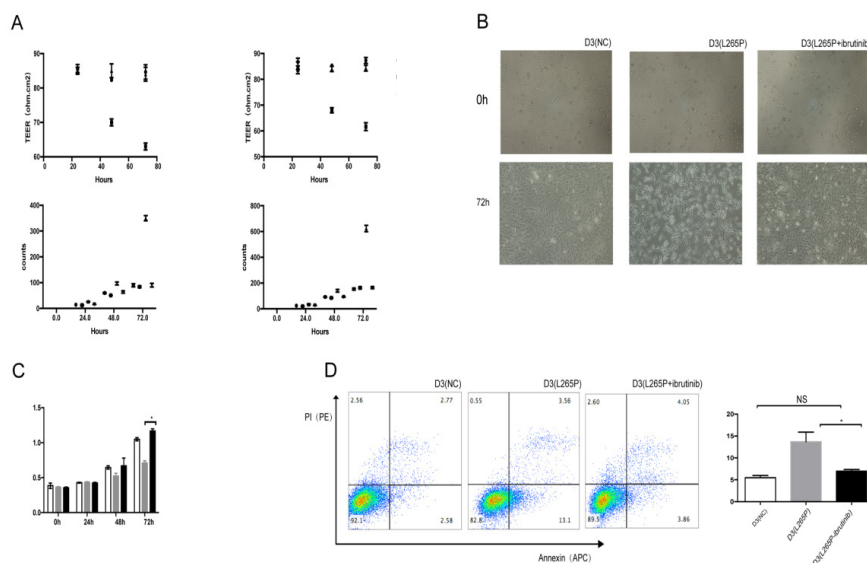


Fig. 3: Ibrutinib made MYD88 L265P lymphoma cells lose the ability to change the biological function of hCMEC/D3 cells, (A): The TEER value of the hCMEC/D3 cells and the numbers of lymphomas that entered the lower chamber; (B): The morphology of hCMEC/D3 cells under microscope; (C): The proliferation of hCMEC/D3 cells tested by CCK8 and (D): Flow cytometry to detect apoptosis of hCMEC/D3 cells
Note: * $p < 0.05$ and * $p < 0.05$, (A) (■): D3 (NC); (■): D3 (L265P); (■): D3 (L265P+ibrutinib); (■): WT; (□): Vector; (■): L265P and (■): L265P+ibrutinib and (C) (□): D3 (NC); (■): D3 (L265P) and (■): D3 (L265P+ibrutinib)

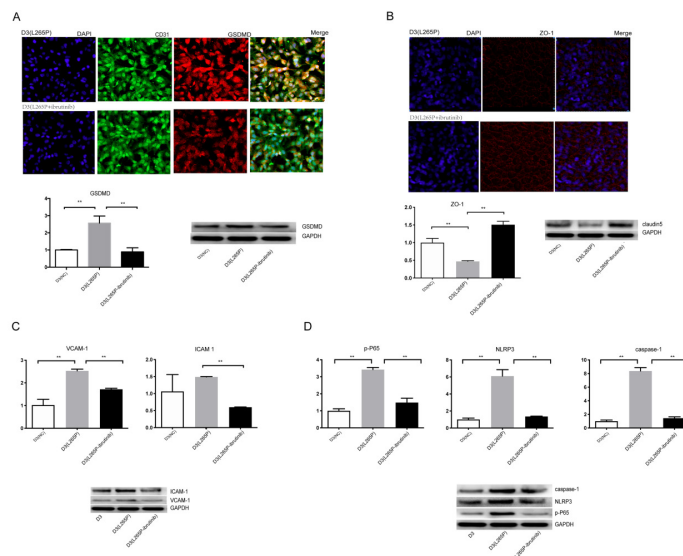


Fig. 4: Ibrutinib inhibited the functions of MYD88 L265P lymphoma cells on the characteristic of hCMEC/D3 cells, (A): Immunofluorescence, RT-PCR and Western blotting analysis of GSDMD in hCMEC/D3 cells for 72 h; (B): Immunofluorescence analysis of ZO-1, RT-PCR analysis of ZO-1 and claudin-5 and Western blot analysis of claudin-5 in hCMEC/D3 cells for 72 h; (C): RT-PCR and Western blotting analysis of ICAM-1 and VCAM-1 in hCMEC/D3 cells and (D): RT-PCR and Western blotting analysis of NF- κ B, NLRP3 and caspase-1 in hCMEC/D3 cells
 Note: ** $p < 0.01$, *** $p < 0.001$, **** $p < 0.0001$ and ** $p < 0.01$

The BBB was the initial and critical filter to prevent metastatic cells from invading the brain. Most metastatic cells could not survive in the brain microenvironment and regenerate the tumors. It is very interesting to study what kind of cells could penetrate the BBB and adapt to the special microenvironment of the CNS to survive. Fukumura *et al.*^[10] suggested that activation of MYD88 might be one of the initial and important genetic alterations of lymphocytes. MYD88-mutant cells could originate outside of the CNS and develop into PCNSL only after undergoing additional alterations, which conferred adaptation to the CNS. In our study, we explored interaction of lymphoma cells and brain microvascular endothelial cells, which were the main constituents of the BBB. The results showed MYD88 L265P lymphoma cells reduced the TEER value of the endothelial cell barrier and increased its permeability. MYD88 L265P lymphoma cells lost the tight junctions of hCMEC/D3 cells, which was convenient to that MYD88 L265P mutation occurred frequently in PCNSL. However, how MYD88 L265P lymphoma cells worked on brain microvascular endothelial cells had not been reported. Mateja *et al.*^[29] discovered that MYD88 L265P was transferred to the cytoplasm of the recipient mast cells and macrophages by Extracellular Vesicles (EVs) from Waldenström's Macroglobulinemia (WM) cells, recruited the endogenous MYD88 which triggered the activation of proinflammatory signaling without

receptor activation. They demonstrated that the binding of MYD88 L265P delivered by EVs to endogenous MYD88 WT lead to enhanced activation of the inflammatory pathway, including the NF- κ B and inflammatory cytokine/chemokine pathway. In our study, we found that MYD88 L265P lymphoma cells affected hCMEC/D3 cells *via* activating NLRP3 and NF- κ B pathway with increased secretion of cytokines. Whether EVs also play an important role in this process deserve future research.

Bruton Tyrosine Kinase (BTK) was a key node in BCR signaling cascades, which mediated signals from BCR to downstream pathways, such as NF- κ B^[30]. MYD88 L265P, not MYD88 WT preferentially formed complexes with phosphorylated BTK (pBTK) in WM cells and the inhibition of either BTK or IRAK1/4 induced WM cell apoptosis^[31]. Our findings suggested that ibrutinib, a covalent irreversible inhibitor of BTK, made MYD88 L265P lymphoma lose the ability to affect the endothelial cells barrier.

The antitumor activity of ibrutinib in r/r PCNSL was considerably greater than reported for patients with r/r DLBCL outside the CNS^[32,33], which mainly attributed to BTK dependence and BCR pathway mutations. For example, the MYD88 mutations were associated with ibrutinib sensitivity in WM and were significantly more common in PCNSL than in DLBCL outside the CNS^[33,34]. Alternatively,

the brain microenvironment might enhance BTK dependence of lymphoma cells through chronic antigen presentation and BCR activation^[35]. Studies had shown that different tumor cells had different affinities for different target organs and these differences depended on the genetic characteristic of the tumor cells. Our study indicated that MYD88 L265P lymphoma cells had a stronger central affinity. Further research needed to determine how genetic and tumor micro environmental factors, alone or in combination, produced the intrinsic BTK dependence of different B cell malignancies.

In summary, CNS lymphoma was rare and with poor prognosis. In this study, we demonstrated that MYD88 L265P lymphoma cells were more aggressive and disrupt the brain microvascular endothelial cells barrier. It manifested by reducing TEER value to increase permeability, down-regulating TJ protein expression to destroy integrity, and increasing LAMs expression to enhance adhesion. This process achieved by inhibiting proliferation and increasing apoptosis and pyrolysis of brain endothelial cells *via* activating NLRP3, caspase-1 and NF- κ B pathway. Ibrutinib made the MYD88 L265P lymphoma cells lose the ability to affect the brain microvascular endothelial cell barrier.

Conflict of interests:

The authors declared no conflict of interests.

REFERENCES

1. Ngo VN, Young RM, Schmitz R, Jhavar S, Xiao W, Lim KH, *et al.* Oncogenically active MYD88 mutations in human lymphoma. *Nature* 2011;470(7332):115-9.
2. Zorofchian S, Lu G, Zhu JJ, Duose DY, Windham J, Esquenazi Y, *et al.* Detection of the MYD88 p. L265P mutation in the CSF of a patient with secondary central nervous system lymphoma. *Front Oncol* 2018;8:382.
3. Rovira J, Karube K, Valera A, Colomer D, Enjuanes A, Colomo L, *et al.* MYD88 L265P mutations, but no other variants, identify a subpopulation of DLBCL patients of activated B-cell origin, extranodal involvement and poor outcome MYD88 mutations (L265P vs. other) in DLBCL. *Clin Cancer Res* 2016;22(11):2755-64.
4. Fernández-Rodríguez C, Bellosillo B, García-García M, Sánchez-González B, Gimeno E, Vela MC, *et al.* MYD88 (L265P) mutation is an independent prognostic factor for outcome in patients with diffuse large B-cell lymphoma. *Leukemia* 2014;28(10):2104-6.
5. Mohile NA, Abrey LE. Primary central nervous system lymphoma. *Neurol Clin* 2007;25(4):1193-207.
6. Hattori K, Sakata-Yanagimoto M, Suehara Y, Yokoyama Y, Kato T, Kurita N, *et al.* Clinical significance of disease-specific MYD88 mutations in circulating DNA in primary central nervous system lymphoma. *Cancer Sci* 2018;109(1):225-30.
7. Braggio E, van Wier S, Ojha J, McPhail E, Asmann YW, Egan J, *et al.* Genome-wide analysis uncovers novel recurrent alterations in primary central nervous system lymphomas. *Clin Cancer Res* 2015;21(17):3986-94.
8. Vater I, Montesinos-Rongen M, Schlesner M, Haake A, Purschke F, Sprute R, *et al.* The mutational pattern of primary lymphoma of the central nervous system determined by whole-exome sequencing. *Leukemia* 2015;29(3):677-85.
9. Yamada S, Ishida Y, Matsuno A, Yamazaki K. Primary diffuse large B-cell lymphomas of central nervous system exhibit remarkably high prevalence of oncogenic MYD88 and CD79B mutations. *Leuk Lymphoma* 2015;56(7):2141-5.
10. Fukumura K, Kawazu M, Kojima S, Ueno T, Sai E, Soda M, *et al.* Genomic characterization of primary central nervous system lymphoma. *Acta Neuropathol* 2016;131:865-75.
11. Hattori K, Sakata-Yanagimoto M, Okoshi Y, Goshima Y, Yanagimoto S, Nakamoto-Matsubara R, *et al.* MYD88 (L265P) mutation is associated with an unfavourable outcome of primary central nervous system lymphoma. *Br J Haematol* 2017;177(3):492-4.
12. Nakamura T, Tateishi K, Niwa T, Matsushita Y, Tamura K, Kinoshita M, *et al.* Recurrent mutations of CD79B and MYD88 are the hallmark of primary central nervous system lymphomas. *Neuropathol Appl Neurobiol* 2016;42(3):279-90.
13. Dubois S, Vially PJ, Bohers E, Bertrand P, Ruminy P, Marchand V, *et al.* Biological and clinical relevance of associated genomic alterations in MYD88 L265P and non-L265P-mutated diffuse large B-cell lymphoma: Analysis of 361 Cases MYD88 L265P and non-L265P DLBCL genomic profiles. *Clin Cancer Res* 2017;23(9):2232-44.
14. Langen UH, Ayloo S, Gu C. Development and cell biology of the blood-brain barrier. *Ann Rev Cell Dev Biol* 2019;35:591-613.
15. Prinz M, Priller J. The role of peripheral immune cells in the CNS in steady state and disease. *Nat Neurosci* 2017;20(2):136-44.
16. Rochfort KD, Collins LE, Murphy RP, Cummins PM. Down regulation of blood-brain barrier phenotype by proinflammatory cytokines involves NADPH oxidase-dependent ROS generation: Consequences for interendothelial adherens and tight junctions. *PloS One* 2014;9(7):e101815.
17. Custodio-Santos T, Videira M, Brito MA. Brain metastasization of breast cancer. *Biochim Biophys Acta Rev Cancer* 2017;1868(1):132-47.
18. Ribelles N, Santonja A, Pajares B, Llácer C, Alba E. The seed and soil hypothesis revisited: Current state of knowledge of inherited genes on prognosis in breast cancer. *Cancer Treat Rev* 2014;40(2):293-9.
19. Minn AJ, Gupta GP, Siegel PM, Bos PD, Shu W, Giri DD, *et al.* Genes that mediate breast cancer metastasis to lung. *Nature* 2005;436(7050):518-24.
20. Bos PD, Zhang XH, Nadal C, Shu W, Gomis RR, Nguyen DX, *et al.* Genes that mediate breast cancer metastasis to the brain. *Nature* 2009;459(7249):1005-9.
21. Shi J, Zhao Y, Wang K, Shi X, Wang Y, Huang H, *et al.* Cleavage of GSDMD by inflammatory caspases determines pyroptotic cell death. *Nature* 2015;526(7575):660-5.
22. Guo Y, Cebelinski E, Matusевич C, Alderisio KA, Lebbad M, McEvoy J, *et al.* Subtyping novel zoonotic pathogen *Cryptosporidium* chipmunk genotype I. *J Clin Microbiol* 2015;53(5):1648-54.
23. Sandoval KE, Witt KA. Blood-brain barrier tight junction permeability and ischemic stroke. *Neurobiol Dis* 2008;32(2):200-19.

24. Hu R, Wang MQ, Ni SH, Wang M, Liu LY, You HY, *et al.* Salidroside ameliorates endothelial inflammation and oxidative stress by regulating the AMPK/NF- κ B/NLRP3 signaling pathway in AGEs-induced HUVECs. *Eur J Pharmacol* 2020;867:172797.
25. Lawrence T. The nuclear factor NF-kappa B pathway in inflammation. *Cold Spring Harb Perspect Biol* 2009;1(6):a001651.
26. Swanson KV, Deng M, Ting JP. The NLRP3 inflammasome: Molecular activation and regulation to therapeutics. *Nat Rev Immunol* 2019;19(8):477-89.
27. Lionakis MS, Dunleavy K, Roschewski M, Widemann BC, Butman JA, Schmitz R, *et al.* Inhibition of B cell receptor signaling by ibrutinib in primary CNS lymphoma. *Cancer Cell* 2017;31(6):833-43.
28. Phelan JD, Young RM, Webster DE, Roulland S, Wright GW, Kasbekar M, *et al.* A multiprotein supercomplex controlling oncogenic signalling in lymphoma. *Nature* 2018;560(7718):387-91.
29. Mateja M, Lainšček D, Benčina M, Chen JG, Romih R, Hunter ZR, *et al.* Extracellular vesicle-mediated transfer of constitutively active MyD88L265P engages MyD88wt and activates signaling. *Blood J Am Soc Hematol* 2018;131(15):1720-9.
30. Young RM, Staudt LM. Targeting pathological B cell receptor signalling in lymphoid malignancies. *Nat Rev Drug Discov* 2013;12(3):229-43.
31. Yang G, Zhou Y, Liu X, Xu L, Cao Y, Manning RJ, *et al.* A mutation in MYD88 (L265P) supports the survival of lymphoplasmacytic cells by activation of Bruton tyrosine kinase in Waldenström macro globulinemia. *Blood* 2013;122(7):1222-32.
32. Grommes C, Pastore A, Palaskas N, Tang SS, Campos C, Schartz D, *et al.* Ibrutinib unmasks critical role of Bruton tyrosine kinase in primary CNS lymphoma ibrutinib in central nervous system lymphoma. *Cancer Discov* 2017;7(9):1018-29.
33. Wilson WH, Young RM, Schmitz R, Yang Y, Pittaluga S, Wright G, *et al.* Targeting B cell receptor signaling with ibrutinib in diffuse large B cell lymphoma. *Nat Med* 2015;21(8):922-6.
34. Treon SP, Tripsas CK, Meid K, Warren D, Varma G, Green R, *et al.* Ibrutinib in previously treated Waldenström's macro globulinemia. *N Engl J Med* 2015;372(15):1430-40.
35. Montesinos-Rongen M, Purschke FG, Brunn A, May C, Nordhoff E, Marcus K, *et al.* Primary central nervous system (CNS) lymphoma B cell receptors recognize CNS proteins. *J Immunol* 2015;195(3):1312-9.

This is an open access article distributed under the terms of the Creative Commons Attribution-NonCommercial-ShareAlike 3.0 License, which allows others to remix, tweak, and build upon the work non-commercially, as long as the author is credited and the new creations are licensed under the identical terms

This article was originally published in a special issue, "Transformative Discoveries in Biomedical and Pharmaceutical Research" Indian J Pharm Sci 2023;85(4) Spl Issue "1-9"